

Carbazole-based 1D and 2D hemicyanines: synthesis, two-photon absorption properties and application for two-photon photopolymerization 3D lithography

Jie Gu,^a Wang Yulan,^{ab} Wei-Qiang Chen,^a Xian-Zi Dong,^a Xuan-Ming Duan^{*ac} and Satoshi Kawata^c

Received (in Montpellier, France) 30th June 2006, Accepted 22nd September 2006

First published as an Advance Article on the web 5th October 2006

DOI: 10.1039/b609309d

One and two dimensional (1D and 2D) carbazole based hemicyanines, where methyl pyridinium, methyl indolium and methyl benzothiazolium were used as acceptor group, were synthesized by Knoevenagel condensation. One-photon absorption, fluorescence and two-photon fluorescence spectra were investigated. The experimental results indicated that the different ionic acceptors affect their one-photon and two-photon properties. Among them, 2D methyl pyridinium carbazole derivatives exhibited low quantum yields and large two-photon absorption cross sections more than 1600 GM. The synthesized compounds were used as photoinitiator of two-photon photopolymerization (TPP), and three-dimensional (3D) microstructure was successfully fabricated by TPP 3D lithography. They could be utilized as effective two-photon polymerization photoinitiators.

Introduction

In the past decade, two-photon absorption (TPA) has attracted increasing attention due to its various applications such as optical data storage, optical power limiting, laser up-conversion, two-photon laser scanning fluorescence microscopy and photodynamic therapy.^{1–5} As one of the most important applications of TPA, 3D micro-fabrication based on two-photon photopolymerization (TPP) has been attracting a great deal of interest due to its possible application in the fields of micro-electromechanical system (MEMS) and 3D photonic devices.^{6–8} Depending on the desired application, chromophores combining a large TPA cross section (δ) and high TPP initiating efficiency, which can favor 3D micro-fabrication processes based on TPP, are needed.

On one hand, some principles for designing TPA materials had been established, while many structural designs of molecules have been estimated for this purpose. Prasad *et al.*^{9–11} have pointed out that 1D D- π -A type molecules containing fluorene or dithienothiophene as the rigid π -conjugate backbone have large δ . Marder *et al.*^{12,13} have demonstrated that symmetric stilbenes containing donor (D) or acceptor (A) groups linked by a π conjugate bridge (D- π -D or A- π -A) exhibit large δ . The structures D- π -A- π -D and A- π -D- π -A are also characterized by large δ . Ray and Leszczynski have found the δ of ionic chromophores to be larger than those of the corresponding neutral molecules.¹⁴ Some ionic chromo-

phores were involved in two-photon absorption studies.^{14–19} Meanwhile, some efforts have proved that 2D and multi-dimensional charge transfer system tend to realize larger δ than the corresponding 1D charge transfer compounds.^{20–22}

On the other hand, hemicyanine system was widely investigated as second-order nonlinear optical materials in related to their large dipole moment and good stability for off-diagonal tensor distribution to first hyperpolarizability (β) and without undesirable losses of transparency in the visible region.²³ Although a number of reports recently showed that 2D intramolecular charge transfer (2D-ICT) organic salts have larger second-order nonlinearities,^{24,25} few efforts have been made to investigate TPA of 2D-ICT organic salts.^{17,18}

Since carbazole is very easy to be modified at the 3- and 6-position to form a C_{2v} symmetric molecule, here, we report C_{2v} symmetric carbazole-based 2D-ICT salts by introducing ionic groups at the 3- and 6-position of carbazole ring, to elongate π -conjugation system compared to its 1D analogue. Within this context, we investigate one-photon and two-photon photophysical properties of 1D-ICT organic salts (**1a–e**) and 2D-ICT organic salts (**2a–e**), where the pyridinium, indolium and benzothiazolium cations were used as acceptor group, the *N*-alkyl-carbazolyl as donor group and a carbon-carbon double bond as π -conjugated bridge. Furthermore the V-shaped 2D-ICT salt **2c** was used in TPP 3D lithography as a photoinitiator.

Experimental

Materials

Carbazole, sodium hydride, trichlorophosphine oxide, methyl iodine, ethyl bromide, pentyl bromide, 2-methyl benzothiazole, 4-methyl pyridine, methyl tosylate, phenyl hydrazine, methyl isopropyl ketone, methyl acrylate and all solvents were

^a Laboratory of Organic Nanophotonics, Technical Institute of Physics and Chemistry, Chinese Academy of Sciences, Beijing, 100080, P. R. China. E-mail: xmduan@mail.ipc.ac.cn; Fax: +86 01 82543597; Tel: +86 10 8254596

^b Department of Chemistry, Beijing University of Chemical Technology, Beijing, 100029, P. R. China

^c Department of Applied Physics, Osaka University, Yamadaoka 2-1, Suita, Osaka, 565-0871, Japan

obtained from Beijing Chemical Reagent Company and used without further purification. Dipentaerythritol hexaacrylate (DEP-6A, trade name: Light Acrylate DEP-6A) was obtained from Kyoeisha Chemical Co., Ltd, Japan.

Instruments and measurements

^1H NMR spectra were recorded on a Varian Gemini-300 spectrometer using CD_3OD as solvent and all shifts are referenced to TMS. The fine splitting of pyridinyl or phenyl ring patterns is ignored and the signals are reported as simple doublets, with J values referring to the two most intense peaks. Mass spectra were measured on Shimadzu LCMS2010. Elemental analyses were performed on Flash EA1112. UV-Visible spectra were obtained on a Shimadzu UV-2550 UV-Vis spectrophotometer. All steady-state fluorescence spectra were measured on a Hitachi F2500 spectrofluorometer. Two-photon induced excited fluorescence (TPEF) spectra were recorded on SD2000 spectrometer (Ocean Optical), excited by a mode-locked Ti-sapphire femtosecond laser (Tsunami, Spectra-Physics) with an oscillating wavelength, pulse width and repetition rate of 780 nm, 80 fs and 82 MHz, respectively.

Two-photon initiated photopolymerization

The same mode-locked Ti-sapphire laser was used in two-photon polymerization 3D lithography. The photocurable resin (PR1) was prepared by mixing 49.9 wt% of methyl acrylate as monomer, 50.0 wt% of DEP-6A as cross-linker and 0.1 wt% of **2c** as photoinitiator. The lasing source was tightly focused by a 100 \times oil-immersion objective lens with a high numerical aperture (N. A. = 1.4, Olympus). The focal point was focused on the liquid photopolymerisable resin which was placed on the xyz-step motorized stage controlled by a computer. After laser fabrication, the unpolymerized resins were washed out using ethanol. The obtained microstructures were characterized with scanning electron microscopy (SEM; Hitachi S-4300FEGd).

Synthesis

The synthetic routes for **1a–e** and **2a–e** are outlined in Scheme 1.

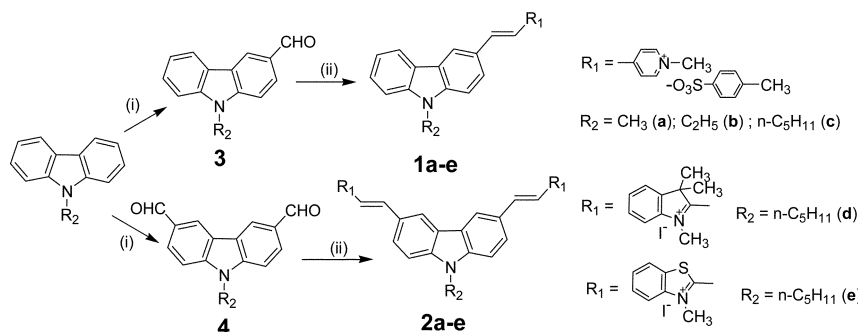
1,4-Dimethyl-pyridinium tosylate (**5**), 1,2,3,3-tetramethyl-indolium iodide (**6**), 1,2-dimethyl benzothiazolium iodide (**7**), *N*-alkyl-carbazole, *N*-alkyl-carbazolyl-3-aldehyde (**3**), *N*-alkyl-carbazolyl-3,6-dialdehydes (**4**) were synthesized according to

literature methods.^{26–28} The compounds **1a–e** and **2a–e** are obtained by Knoevenagel condensation.²⁷ The typical procedure for **1a–e** and **2a–e** is: salt **5** (10 mmol) and aldehyde **3** (10 mmol) were added to a 50 mL flask with 25 mL ethanol, followed by catalytic piperidine (1.0 mL). The resulting mixture was allowed to stir overnight. After concentration, the residue was recrystallized from acetonitrile–diethyl ether, further recrystallization gives the desired product. When a pentyl group was introduced at the 9-position, the solubility increased and further recrystallization is needed to afford purified products.

3-[2-(1-Methylpyridinium)vinyl]-9-methyl-carbazole tosylate (1a). Yield: 41%. Mp 241–242 °C. ^1H NMR (CD_3OD , δ/ppm): 8.52 (d, 2 H, $J = 6.8$ Hz), 8.43 (s, 1 H), 8.14 (d, 1 H, $J = 7.9$ Hz), 8.03 (d, 1 H, $J = 16.5$ Hz), 8.00 (d, 2 H, $J = 6.8$ Hz), 7.87 (d, 1 H, $J = 7.9$ Hz), 7.71 (d, 2 H, $J = 7.9$ Hz), 7.56 (d, 1 H, $J = 8.6$ Hz), 7.52 (m, 2 H), 7.30 (d, 1 H, $J = 16.5$ Hz), 7.27 (t, 1 H, $J = 8.6$ Hz), 7.22 (d, 2 H, $J = 7.9$ Hz), 4.19 (s, 3 H), 3.90 (s, 3 H), 2.34 (s, 3 H). Anal. calcd for $\text{C}_{28}\text{H}_{26}\text{N}_2\text{O}_3\text{S}$: C, 71.46; H, 5.57; N, 5.95; found: C, 71.29; H, 5.62; N, 5.99%.

3-[2-(1-Methylpyridinium)vinyl]-9-ethyl-carbazole tosylate (1b). Yield: 31%. Mp 241–243 °C. ^1H NMR (CD_3OD , δ/ppm): 8.52 (d, 2 H, $J = 6.8$ Hz), 8.43 (s, 1 H), 8.14 (d, 1 H, $J = 7.9$ Hz), 8.03 (d, 1 H, $J = 16.5$ Hz), 8.00 (d, 2 H, $J = 6.8$ Hz), 7.87 (d, 1 H, $J = 7.9$ Hz), 7.71 (d, 2 H, $J = 7.9$ Hz), 7.56 (d, 1 H, $J = 8.6$ Hz), 7.52 (m, 2 H), 7.30 (d, 1 H, $J = 16.5$ Hz), 7.27 (t, 1 H, $J = 8.6$ Hz), 7.22 (d, 2 H, $J = 7.9$ Hz), 4.46 (q, 2 H), 4.18 (s, 3 H), 2.34 (s, 3 H), 1.42 (t, 3 H). Anal. calcd for $\text{C}_{29}\text{H}_{28}\text{N}_2\text{O}_3\text{S}$: C, 71.87; H, 5.82; N, 5.78; found C, 71.39; H, 5.79; N, 5.98%.

3-[2-(1-Methylpyridinium)vinyl]-9-pentyl-carbazole tosylate (1c). Yield: 15%. Mp 241–242 °C. ^1H NMR (CD_3OD , δ/ppm): 8.52 (d, 2 H, $J = 6.8$ Hz), 8.43 (s, 1 H), 8.14 (d, 1 H, $J = 7.9$ Hz), 8.03 (d, 1 H, $J = 16.5$ Hz), 8.00 (d, 2 H, $J = 6.8$ Hz), 7.87 (d, 1 H, $J = 7.9$ Hz), 7.71 (d, 2 H, $J = 7.9$ Hz), 7.56 (d, 1 H, $J = 8.6$ Hz), 7.52 (m, 2 H), 7.30 (d, 1 H, $J = 16.5$ Hz), 7.27 (t, 1 H, $J = 8.6$ Hz), 7.22 (d, 2 H, $J = 7.9$ Hz), 4.46 (t, 2 H), 4.18 (s, 3 H), 2.34 (s, 3 H), 1.88 (m, 2 H), 1.37 (m, 4 H), 0.88 (t, 3 H). Anal. calcd for $\text{C}_{32}\text{H}_{34}\text{N}_2\text{O}_3\text{S} \cdot \text{H}_2\text{O}$: C, 70.56; H, 6.66; N, 5.14; found: C, 70.90; H, 6.85; N, 4.92%.



Scheme 1 Synthetic route to **1a–e** and **2a–e**. Reagents and conditions: (i) POCl_3/DMF , $\text{ClCH}_2\text{CH}_2\text{Cl}$, reflux; (ii) salts **5–7**, piperidine (catalytic amount), ethanol, reflux.

3-[2-(1',3',3'-Thiomethyl-indolium-2'-yl)vinyl]-9-pentyl-carbazole iodide (1d). Yield: 45%. Mp 119–122 °C. ^1H NMR (CD_3OD , δ/ppm): 0.89 (m, 3 H), 1.39 (m, 4 H), 1.61 (m, 2 H), 1.92 (s, 6 H), 4.18 (m, 2 H), 4.49 (s, 3 H), 7.37 (m, 1 H), 7.68 (m, 8 H), 8.22 (d, $J = 8.7$ Hz, 1 H), 8.28 (d, $J = 7.6$ Hz, 1 H), 8.67 (d, $J = 15.9$ Hz, 1 H), 8.94 (s, 1 H); MS (m/z): 421.6 $[\text{M-I}]^+$; Anal. calcd for $\text{C}_{30}\text{H}_{33}\text{IN}_2 \cdot \text{H}_2\text{O}$: C, 63.60; H, 6.23; N, 4.94; found: C, 63.44; H, 6.10; N, 5.00%.

3-[2-(1'-Methylbenzothiazolium-2'-yl)vinyl]-9-pentyl-carbazole iodide (1e). Yield: 55%. Mp 233–235 °C. ^1H NMR (DMSO-D_6 , δ/ppm): 0.87 (t, $J = 6.4$ Hz, 3 H), 1.31 (m, 2 H), 1.57 (m, 2 H), 1.71 (m, 2 H), 3.90 (t, $J = 7.0$ Hz, 2 H), 4.22 (s, 3 H), 6.94 (m, 1 H), 7.13 (d, $J = 8.0$ Hz, 1 H), 7.30 (m, 4 H), 7.42 (dd, $J_1 = 7.2$ Hz, $J_2 = 7.5$ Hz, 1 H), 7.66 (s, $J = 8.7$ Hz, 1 H), 8.10 (d, $J = 15.3$ Hz, 1 H), 8.27 (d, $J = 8.4$ Hz, 1 H), 8.38 (d, $J = 15.5$ Hz, 1 H), 8.57 (d, $J = 7.6$ Hz, 1 H), 9.25 (s, 1 H). MS (m/z): 411.5 $[\text{M-I}]^+$.

3,6-Bis[2-(1-methylpyridinium)vinyl]-9-methyl-carbazole di-tosylate (2a). Yield: 37%. Mp >280 °C. ^1H NMR (CD_3OD , δ/ppm): 8.64 (d, 4 H, $J = 6.4$ Hz), 8.59 (s, 2 H), 8.14 (d, 2 H, $J = 15.8$ Hz), 8.13 (d, 4 H, $J = 6.4$ Hz), 7.97 (d, 2 H, $J = 8.6$ Hz), 7.71 (d, 4 H, $J = 7.8$ Hz), 7.66 (d, 2 H, $J = 8.6$ Hz), 7.49 (d, 2 H, $J = 15.8$ Hz), 7.21 (d, 4 H, $J = 7.8$ Hz), 4.28 (s, 6 H), 3.97 (s, 3 H), 2.33 (s, 6 H). MS (m/z): 588.4 $[\text{M-171.0}]^+$, 208.8 $[\text{M-2} \times 171.0]^{2+}$, 171.0 [tosylate] $^-$ (calcd for $\text{C}_{43}\text{H}_{41}\text{N}_3\text{O}_6\text{S}_2$ 759.2). Anal. calcd for $\text{C}_{43}\text{H}_{41}\text{N}_3\text{O}_6\text{S}_2 \cdot (\text{H}_2\text{O})_{0.5}$: C, 67.17; H, 5.51; N, 5.46; found C, 67.14; H, 5.43; N, 5.43%.

3,6-Bis[2-(1-methylpyridinium)vinyl]-9-ethyl-carbazole di-tosylate (2b). 31% yield. Mp 245–246 °C. ^1H NMR (CD_3OD , δ/ppm): 8.61 (d, 4 H, $J = 6.5$ Hz), 8.58 (s, 2 H), 8.12 (d, 2 H, $J = 15.9$ Hz), 8.09 (d, 4 H, $J = 6.5$ Hz), 7.91 (d, 2 H, $J = 8.6$ Hz), 7.71 (d, 4 H, $J = 8.6$ Hz), 7.62 (d, 2 H, $J = 8.6$ Hz), 7.40 (d, 2 H, $J = 15.9$ Hz), 7.21 (d, 4 H, $J = 8.6$ Hz), 4.46 (q, 2 H), 4.18 (s, 3 H), 2.34 (s, 3 H), 1.42 (t, 3 H). Anal. calcd for $\text{C}_{44}\text{H}_{43}\text{N}_3\text{O}_6\text{S}_2 \cdot (\text{H}_2\text{O})_2$: C, 65.24; H, 5.85; N, 5.19; found C, 65.60; H, 6.05; N, 5.37%.

3,6-Bis[2-(1-methylpyridinium)vinyl]-9-pentyl-carbazole di-tosylate (2c). 14% yield. Mp 256–259 °C. ^1H NMR (CD_3OD , δ/ppm): 8.61 (d, 4 H, $J = 6.5$ Hz), 8.58 (s, 2 H), 8.12 (d, 2 H, $J = 15.9$ Hz), 8.09 (d, 4 H, $J = 6.5$ Hz), 7.91 (d, 2 H, $J = 8.6$ Hz), 7.71 (d, 4 H, $J = 8.6$ Hz), 7.62 (d, 2 H, $J = 8.6$ Hz), 7.40 (d, 2 H, $J = 15.9$ Hz), 7.21 (d, 4 H, $J = 8.6$ Hz), 4.43 (t, 2 H), 4.25 (s, 6 H), 2.31 (s, 6 H), 1.87 (m, 2 H), 1.37 (m, 4 H), 0.87 (t, 3 H). MS (m/z): 644.5 $[\text{M-171.0}]^+$, 237.0 $[\text{M-2} \times 171.0]^{2+}$, 171.0 [tosylate] $^-$ (calcd for $\text{C}_{47}\text{H}_{49}\text{N}_3\text{O}_6\text{S}_2$ 815.3). Anal. calcd for $\text{C}_{47}\text{H}_{49}\text{N}_3\text{O}_6\text{S}_2 \cdot (\text{H}_2\text{O})_{0.5}$: C, 68.42; H, 6.11; N, 5.09; found C, 68.12; H, 6.05; N, 5.20%.

3,6-Bis[2-(1',3',3'-thiomethyl-indolium-2'-yl)vinyl]-9-pentyl-carbazole diiodide (2d). 72% yield. Mp >300 °C. ^1H NMR (CD_3OD , δ/ppm): 0.91 (m, 3 H), 1.41 (m, 4 H), 1.61 (m, 2 H), 1.94 (s, 12 H), 4.31 (m, 2 H), 4.57 (s, 6 H), 7.65 (m, 6 H), 7.84 (m, 6 H), 8.25 (d, $J = 8.7$ Hz, 2 H), 8.67 (d, $J = 15.7$ Hz, 2 H), 9.49 (s, 2 H). MS (m/z): 605.6 $[\text{M-2I}]^+$, 732.6 $[\text{M-I}]^+$. Anal. calcd for $\text{C}_{43}\text{H}_{47}\text{I}_2\text{N}_3$: C, 60.08; H, 5.51; N, 4.89; found: C, 60.85; H, 5.65; N, 4.88%.

3,6-Bis[2-(N-methylbenzothiazolium-2-yl)vinyl]-9-pentyl-carbazole diiodide (2e). 65% yield. Mp 252–254 °C. ^1H NMR (DMSO-D_6 , δ/ppm): 0.81 (t, $J = 6.0$ Hz, 3 H), 1.30 (m, 4 H), 1.80 (m, 2 H), 4.40 (s, 3 H), 4.54 (m, 2 H), 7.77 (t, $J = 7.6$ Hz, 2 H), 7.88 (dd, $J = 8.8$ Hz, $J = 7.7$ Hz, 4 H), 8.11 (d, $J = 15.7$ Hz, 2 H), 8.23 (d, $J = 8.4$ Hz, 2 H), 8.31 (d, $J = 8.6$ Hz, 2 H), 8.42 (d, $J = 16.2$ Hz, 2 H), 8.44 (m, 2 H), 9.04 (s, 2 H). MS (m/z): 587.3 $[\text{M-2I}]^+$, 712.5 $[\text{M-I}]^+$. Anal. calcd for $\text{C}_{37}\text{H}_{35}\text{I}_2\text{N}_3\text{S}_2$: C, 52.93; H, 4.20; N, 5.00; found: C, 52.93; H, 4.33; N, 4.96%.

Results and discussion

One-photon optical properties

The normalized one-photon absorption and fluorescence spectra of **1c–e** and **2c–e** are shown in Fig. 1. The absorption spectra of **2c–e** exhibit one weaker shoulder peak but the spectra of **1c–e** do not. The lowest excited band and the second excited band of **2c–e** observed are derived from the strong interaction between two branched components similar to **1c–e**. The absorption maximum of 1D-ICT system is red shifted

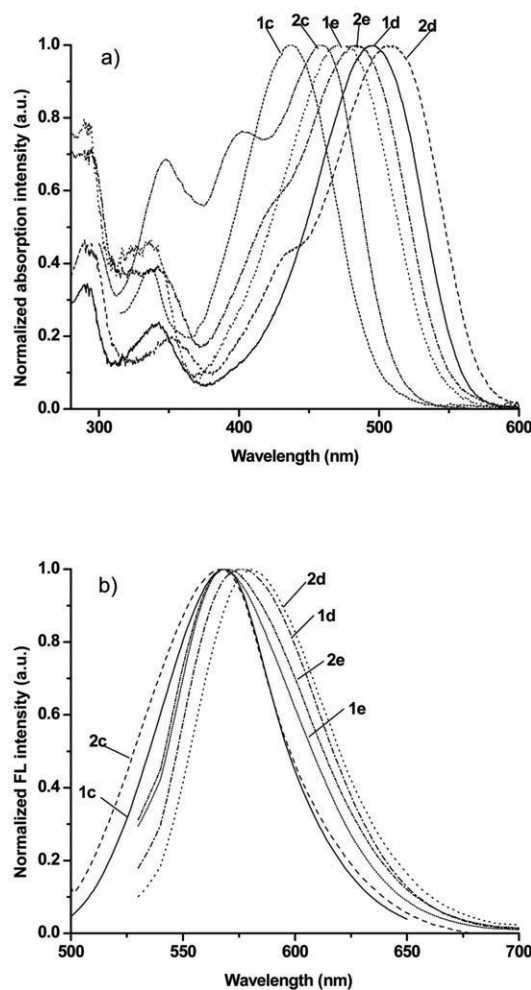


Fig. 1 Normalized Vis-UV spectra (a) and fluorescence spectra (b) of **1c–e** and **2c–e**. Excited wavelength at 500 nm for **1c/2c**, 530 nm for **1d/2d** and **1e/2e**.

from 437 to 495 nm as the acceptor changed from pyridinium (**1c**) to indolium (**1d**). The same phenomenon is observed for the 2D system, with an absorption maximum of 458 nm for **2c**, 495 nm for **2e**, and 510 nm for **2d**.

As shown in Fig. 1(b), the fluorescence of indolium compounds show a red shift compared to pyridinium compounds. It is worth noting that the fluorescence spectrum of **2d** is red shifted 5 nm compared to **1d** for indolium derivatives, however another two couples exhibit nearly the same fluorescence spectra. With regard to the indolium cation, the acceptor is so strong that it affects the degree of intramolecular charge transfer of the 2D compound in its excited state. The energy of the 2D-ICTs is in the order of **2c** > **2e** > **2d**, which means that indolium is the strongest acceptor and pyridinium is the weakest among these three cations.

The fluorescence quantum yields were measured at concentrations of $\sim 1\text{--}2 \times 10^{-6}$ M according to the following expression with fluorescein in 0.1 M aqueous NaOH solution as a reference standard ($\Phi = 0.90$) (eqn (1)).^{29,30}

$$\Phi_s = \Phi_r \left(\frac{A_r(\lambda_r)}{A_s(\lambda_s)} \right) \left(\frac{I_r(\lambda_r)}{I_s(\lambda_s)} \right) \left(\frac{n_s^2}{n_r^2} \right) \left(\frac{F_s}{F_r} \right) \quad (1)$$

Φ is the quantum yield, n is the refractive index, $I(\lambda)$ is the relative intensity of exciting light at wavelength λ , $A(\lambda)$ is the absorbance of solution at the exciting wavelength λ , and F is the integrated area under the emission spectrum. Subscripts s and r refer to the sample and reference solution, respectively.

All the one-photon photophysical data are listed in Table 1. The excitation and emission show no significant dependence on chain length at the substituted carbazolyl nitrogen. The quantum yields of 1D compounds are larger than those of the corresponding 2D compounds in methanol. The quantum yields can be improved using high viscosity solvents,³¹ those of **2c** and **2d** in glycerol increase to 7.7 and 7.6% from 1.3 and 0.7% in methanol, respectively.

Two-photon absorption properties

The two-photon induced fluorescence emission spectra of **1c–d** and **2c–e** are presented in Fig. 2. Compare to their one photon excited fluorescence, all TPEF of these compounds are red

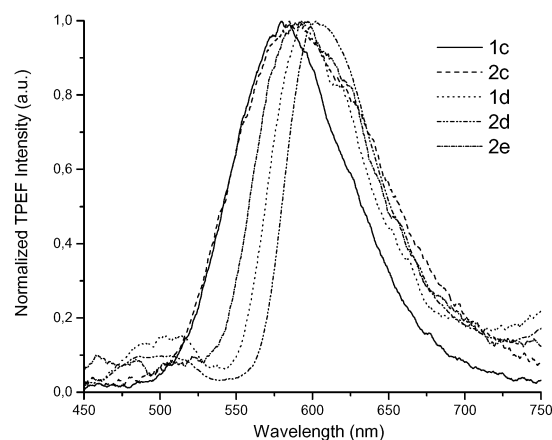


Fig. 2 The normalized two-photon induced fluorescence emission spectra of **1c–d** and **2c–e** excited at 820 nm.

shifted 14–20 nm which may be due to the effect of reabsorption in the higher concentration of 10^{-4} M. Fig. 3 presents the relationship of input power and output fluorescence intensity under the two-photon induced excitation. The fluorescence intensity is nearly linear to input power I_{in}^2 with very good fitting ($R = 0.9999$), which provides clear evidence to confirm that the fluorescence is derived from two-photon induced excitation of these compounds.

TPA cross sections were determined by the two-photon-induced excited fluorescence (TPEF) method.³² It is assumed that the quantum efficiencies after two-photon excitation are the same as those after one-photon excitation. The TPA cross sections are obtained *via* the TPEF method with calibration against fluorescein with a known $\Phi\delta$ value in aqueous NaOH solution (pH 11) at concentrations of 1.0×10^{-4} M for the measurement by using femtosecond pulse laser as the excitation resource. The samples were dissolved in solvents at concentrations of $\sim 1\text{--}2 \times 10^{-4}$ M. To ensure that the measured signals were solely due to TPA, the dependence of TPEF on the incident intensity was verified in each case to be quadratic.

Table 1 Photophysical data of **1** and **2** at room temperature in methanol

	λ_{abs}/nm	$\epsilon_{max}^a/M^{-1} cm^{-1}$	λ_{em}/nm	ST^b/cm^{-1}	Φ^c	λ_{max}^{TPAd}/nm	$\Phi\delta^e$	δ^f/GM
1a	435	27 800	568	5383	0.11	880	52.6	470
1b	435	26 100	568	5383	0.096	880	47.0	490
1c	437	25 800	568	5278	0.090	880	41.0	456
1d	495	42 300	575	2811	0.019	—	—	—
					0.034 ^g	880	6.9 ^g	203 ^g
1e	474	23 700	569	3522	0.061	ND	ND	ND
2a	456	57 550	568	4324	0.011	800	19.1	1737
2b	456	55 430	568	4324	0.013	810	22.6	1740
2c	458	57 500	569	4259	0.013	800	21.5	1650
					0.077 ^g	800	115 ^g	1495 ^g
2d	510	40 300	581	2396	0.007	—	—	—
					0.076 ^g	880	36 ^g	474 ^g
2e	495	87 100	570	2658	0.039	840	5.9	151

^a Molar absorption coefficient. ^b Stokes shift $ST = (1/\lambda_{abs}) - (1/\lambda_{em})$. ^c Fluorescence quantum yield in methanol determined relative to fluorescein in 0.1 M NaOH. ^d The wavelength of the TPA maximum in the range 790–880 nm. ^e Two photon emission cross section. ^f TPA cross section, 1 GM = $10^{-50} cm^4 s photon^{-1}$. ^g Measured in glycerol. ND not detected.

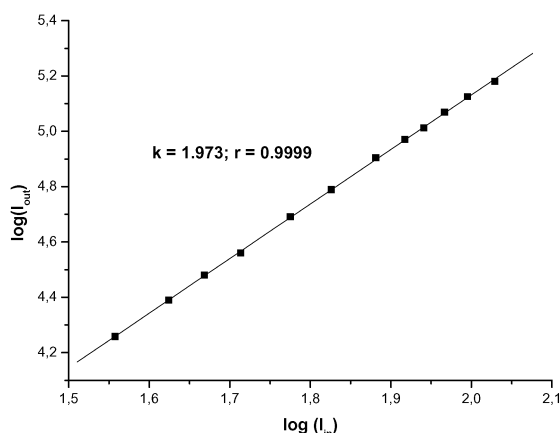


Fig. 3 The relationship of input intensity and output intensity during the TPA cross section measurements for **1c**. The solid squares are experimental spots and solid line is the fitting line.

Then the TPA cross section δ were calculated on the basis of the following expression (eqn (2))

$$\delta_s = \delta_r \frac{C_r n_r F_s \Phi_r}{C_s n_s F_r \Phi_s} \quad (2)$$

δ is TPA cross section, C and n are the concentration and refractive index of the sample solution, F is the integrated area under the TPEF spectrum, and Φ is the fluorescence quantum yield. Subscripts s and r refer to the sample and reference solution, respectively.

The shifts of TPA cross section of **1c–d** and **2c–e** upon excitation by wavelengths from 790–880 nm were presented in Fig. 4. The TPA maxima below 880 nm appear at around 800 nm for **2a–c** with the TPA cross sections $\delta = 1737, 1740, 1650$ GM, respectively; 880 nm for **2d** with $\delta = 474$ GM and 840 nm for **2e** with $\delta = 151$ GM, which are contrasted to the shoulder peak as the second intramolecular charge transfer state. It is clearly shown that the second ICT state gives great contributions to TPA spectrum for 2D-ICT molecules. The TPA excited emission maximum and the TPA cross section maximum of these compounds were summarized in Table 1.

Two-photon initiated photopolymerization

As shown above, compound **2c** possesses a large TPA cross section in the range of 780–820 nm which is widely used in 3D laser microlithography. In order to investigate the two-photon photosensitivity of chromophore **2c**, the threshold energy of polymerization was evaluated by analyzing the polymer spots produced by single-spot exposures. The threshold power for **2c** in PR1 is 3.0 mW.

The microstructure with high spatial resolution was successfully fabricated by using induced laser power of 10 mW with exposure time of 2 ms. A microstructure of diamond-lattice photonic crystal³³ with a single-layer 8×8 lattice was successfully fabricated, the SEM image of this is illustrated in Fig. 5. Usually, 1–5 wt% of photoinitiator in resins have been used for photopolymerization,³⁴ however, only 0.1 wt% of **2c** was mixed in our experiments. This result clearly indicated that **2c** is a photoinitiator with high TPP initiating efficiency. In our previous study on stilbazolium cations using semiempirical

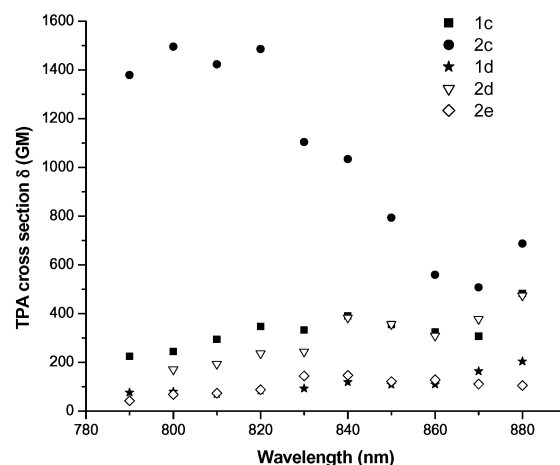


Fig. 4 The TPA cross sections of **1c–d** and **2c–e** at different wavelengths.

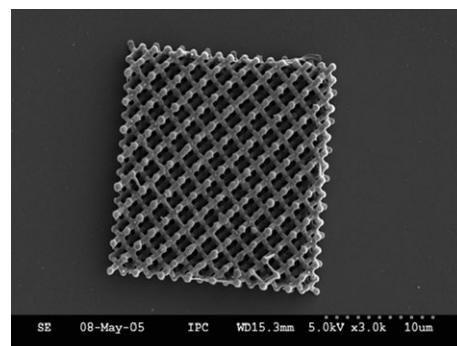


Fig. 5 SEM image of 3D diamond photonic crystal microstructure.

calculations,³⁵ we found that stilbazolium cations are easily excited to obtain a diradical conformation in their excited state. The high TPP initiating efficiency of **2c** should be due to the diradical form of the stilbazolium structure.

Conclusions

In conclusion, C_{2v} symmetric carbazole-based 2D hemicyanines compounds as well as their 1D analogues were synthesized, and their one photon absorption, steady state fluorescence, TPA and TPEF were investigated. The results showed that the 2D systems possessed larger TPA cross sections than the 1D systems although the 1D systems have higher fluorescence quantum yields. The threshold of TPP for the C_{2v} symmetric carbazole-based 2D stilbazolium compound, 3,6-bis[2-(1-methylpyridinium) vinyl]-9-pentyl-carbazole ditosylate (**2c**) was determined to be 3.0 mW and it was successfully used as TPP photoinitiator for TPP microfabrication.

Acknowledgements

This work was supported in part from the “One Hundred Overseas Talents Program” of the Chinese Academy of Sciences (CAS) and the “Nonlinear Nanophotonics” Project of Japan Science and Technology Agency (JST).

References

- 1 S. Kawata and Y. Kawata, *Chem. Rev.*, 2000, **100**, 1777.
- 2 K. D. Belfield, K. J. Schafer, Y. Liu, J. Liu, X. B. Ren and E. W. Van Stryland, *J. Phys. Org. Chem.*, 2000, **13**, 837.
- 3 Denk, W. Strickler, J. H. Webb and W. W., *Science*, 1990, **248**, 73.
- 4 R. H. Kohler, J. Cao, W. R. Zipfel, W. W. Webb and M. R. Hansen, *Science*, 1997, **276**, 2039.
- 5 M. J. Miller, S. H. Wei, I. Parker and M. D. Cahalan, *Science*, 2002, **296**, 1869.
- 6 S. Kawata, H.-B. Sun, T. Tanaka and K. Takada, *Nature*, 2001, **412**, 697.
- 7 B. H. Cumpston, S. P. Ananthavel, S. Barlow, D. L. Dyer, J. E. Ehrlich, L. L. Erskine, A. A. Heikal, S. M. Kuebler, I. Y. S. Lee, D. McCord-Maughon, J. Q. Qin, H. Rockel, M. Rumi, X. L. Wu, S. R. Marder and J. W. Perry, *Nature*, 1999, **398**, 51.
- 8 T.-C. Lin, S. J. Chung, K.-S. Kim, X.-P. Wang, G.-S. He, J. Swiatkiewicz, H. E. Pudavar and P. N. Prasad, *Adv. Polym. Sci.*, 2003, **161**, 157.
- 9 B. A. Reinhardt, L. L. Brott, S. J. Clarkson, A. G. Dillard, J. C. Bhatt, R. Kannan, L. Yuan, G. S. He and P. N. Prasad, *Chem. Mater.*, 1998, **10**, 1863.
- 10 R. Kannan, G. S. He, L. Yuan, F. Xu, P. N. Prasad, A. G. Dombroskie, B. A. Reinhardt, J. W. Baur, R. A. Vaia and L.-S. Tan, *Chem. Mater.*, 2001, **13**, 1896.
- 11 O.-K. Kim, K.-S. Lee, H. Y. Woo, K.-S. Kim, G. S. He, J. Swiatkiewicz and P. N. Prasad, *Chem. Mater.*, 2000, **12**, 284.
- 12 M. Rumi, J. E. Ehrlich, A. A. Heikal, J. W. Perry, S. Barlow, Z. Hu, D. McCord-Maughon, T. C. Parker, H. Röckel, S. Thayumanavan, S. R. Marder, D. Beljonne and J.-L. Brédas, *J. Am. Chem. Soc.*, 2000, **122**, 9500.
- 13 M. Albota, D. Beljonne, J.-L. Brédas, J. E. Ehrlich, J.-Y. Fu, A. A. Heikal, S. E. Hess, T. Kogej, M. D. Levin, S. R. Marder, D. McCord-Maughon, J. W. Perry, H. Röckel, M. Rumi, G. Subramaniam, W. W. Webb, X.-L. Wu and C. Xu, *Science*, 1998, **281**, 1653.
- 14 P. C Ray and J. Leszczynski, *J. Phys. Chem. A*, 2005, **109**, 6689.
- 15 C. F. Zhao, G. S. He, J. D. Bhawalkar, C. K. Park and Paras N. Prasad, *Chem. Mater.*, 1995, **7**, 1979.
- 16 Y. F. Zhou, F. P. Meng, X. Zhao, S. Y. Feng and M. H. Jiang, *Chem. Phys.*, 2001, **269**, 441.
- 17 K. Kamada, K. Ohta, Y. Iwase and K. Kondo, *Chem. Phys. Lett.*, 2003, **372**, 386.
- 18 A. Abboto, L. Beverina, R. Bozio, A. Facchetti, C. Ferrante, G. A. Pagani, D. Pedron and R. Signorini, *Org. Lett.*, 2002, **4**, 1495.
- 19 X. M. Wang, D. Wang, G. Y. Zhou, W. T. Yu, Y. F. Zhou, Q. Fang and M. H. Jiang, *J. Mater. Chem.*, 2001, **11**, 1600.
- 20 L. Porres, O. Mongin, C. Katan, M. Charlot, T. Pons, J. Mertz and M. Blanchard-Desce, *Org. Lett.*, 2004, **6**, 47.
- 21 M. Drobizhev, A. Karotki, Y. Dzenis, A. Rebane, Z. Suo and C. W. Spangler, *J. Phys. Chem. B*, 2003, **107**, 7540.
- 22 S.-J. Chung, K.-S. Kim, T.-C. Lin, G. S. He, J. Swiatkiewicz and P. N. Prasad, *J. Phys. Chem. B*, 1999, **103**, 10741.
- 23 X.-M. Duan, H. Konami, S. Okada, H. Oikawa, H. Matsuda and H. Nakanishi, *J. Phys. Chem.*, 1996, **100**, 17780.
- 24 B. J. Coe, J. A. Harris, B. S. Brunshwig, J. Garin and J. Orduna, *J. Am. Chem. Soc.*, 2005, **127**, 3284.
- 25 B. J. Coe, J. A. Harris, L. A. Jones, B. S. Brunshwig, K. Song, K. Clays, J. Garin, J. Orduna, S. J. Coles and M. B. Hursthouse, *J. Am. Chem. Soc.*, 2005, **127**, 4845.
- 26 W. J. Kuo, G. H. Hsiue and R. J. Jeng, *Macromolecules*, 2001, **34**, 2373.
- 27 B. J. Coe, J. A. Harris, I. Asselberghs, K. Clays, G. Olbrechts, A. Persoons, J. T. Hupp, R. C. Johnson, S. J. Coles, M. B. Hursthouse and K. Nakatani, *Adv. Funct. Mater.*, 2002, **12**, 110.
- 28 Y. Zhang, L. Wang, T. Wada and H. Sasabe, *Macromolecules*, 1996, **29**, 1569.
- 29 J. N. Demas and G. A. Crosby, *J. Phys. Chem.*, 1971, **75**, 991.
- 30 R. A. Velapoldi and H. H. Tonnesen, *J. Fluoresc.*, 2004, **14**, 465.
- 31 Y. Y. Huang, T. R. Cheng, F. Y. Li, C. P. Luo, C.-H. Huang, Z. G. Cai, X. R. Zeng and J. Y. Zhou, *J. Phys. Chem. B*, 2002, **106**, 10031.
- 32 C. Xu and W. W. Webb, *J. Opt. Soc. Am. B*, 1996, **13**, 481.
- 33 K. Kaneko, H. B. Sun, X.-M. Duan and S. Kawata, *Appl. Phys. Lett.*, 2003, **83**, 2091.
- 34 L. H. Nguyen, M. Straub and M. Gu, *Adv. Funct. Mater.*, 2005, **15**, 209.
- 35 X.-M. Duan, T. Wada, S. Okada, H. Oikawa, H. Sasabe and H. Nakanishi, *MRS Symp. Proc.*, 2000, **581**, B.3.31-1-6.